Bypassing the Nitrido Wall Using a Redox-Active Isocyanide: Nucleophilic Attack on CO by a Rhenium Nitride Complex

Alexander S. Hegg,[a],+ Ryan S. Donnelly,[a],+ Jeremy E. Weber,[a],+ Robert H. Crabtree,[a] Brandon Q. Mercado,[a] and Patrick L. Holland [a],*

[a] A. S. Hegg, R. S. Donnelly, J. E. Weber, R. H. Crabtree, B. Q. Mercado, P. L. Holland
Department of Chemistry
Yale University
225 Prospect St., New Haven, Connecticut, USA
E-mail: patrick.holland@yale.edu
+ Co-First Authors

Abstract: Reactive rhenium(III) nitride complexes could result from filling Re–N π* orbitals, but such complexes lie beyond the "nitrido wall" and are rare due to their instability. Here, we describe a method for bypassing the nitrido wall by incorporating a redox-active isocyanide supporting ligand, which accommodates two electrons as shown by crystallographic, spectroscopic, and computational studies. These electrons can be returned to the metal during its facile reaction with CO to form a cyanate complex, demonstrating the nucleophilic reactivity of the nitride. Thus, assistance by the isocyanide enables an N_2-derived rhenium nitride to engage in N–C bond forming reactivity.

Introduction

Terminal nitride complexes are crucial intermediates in N_2 reduction and NH_3 oxidation sequences by systems with metals in groups 6-8.[1] However, terminal nitride complexes of these metals often form strong M–N triple bonds that resist functionalization, limiting their reactivity.[1e, 2] In order to design catalysts with nitrides as intermediates, it is essential to make these nitride ligands more reactive, and to understand the factors that determine the strength of the M–N bonds.

The bonding in metal–nitride multiple bonds is typically described by the Gray−Ballhausen (GB) model, which focuses on the π bond order of tetragonal complexes with a oxo or nitride in the apical position.[3] As shown at the left of Figure 1, when a complex has a square pyramidal (SQPY) geometry, the lowest-energy d orbital is nonbonding; thus it can accommodate a maximum of 2 d electrons without occupying π* orbitals that would weaken the metal-nitride interaction. Therefore, it is rare to find terminal nitrides with a tetragonal geometry that have more than two d electrons, which has been termed the "nitrido wall."[4] A SQPY, d^3 ruthenium(V) nitride complex has been reported, although its electronic structure was not discussed.[5] Additionally, a transient SQPY d^3 iron(V) nitride intermediate has been implicated in a nitride oxygenation reaction.[6] Since these complexes break through the nitrido wall, they are unstable and highly reactive but more remains to be learned about their electronic structures and properties.

Square planar (SQPL) and tetrahedral (Td) geometries have different metal-based frontier orbitals, which are shown in the center and right of Figure 1.[7] In these geometries, 4 d electrons can be accommodated in nonbonding orbitals, but d-electron counts higher than this weaken the metal-nitride bond. Thus, the nitrido wall is shifted. Breaking through this wall is also rare, but Schneider and co-workers reported a square planar iridium(IV)–nitrido complex with a d^5 configuration which was highly reactive.[7] Electronic structure studies revealed that a M–$N_{nitride}$ π* orbital is the SOMO, giving radical character on the nitride.

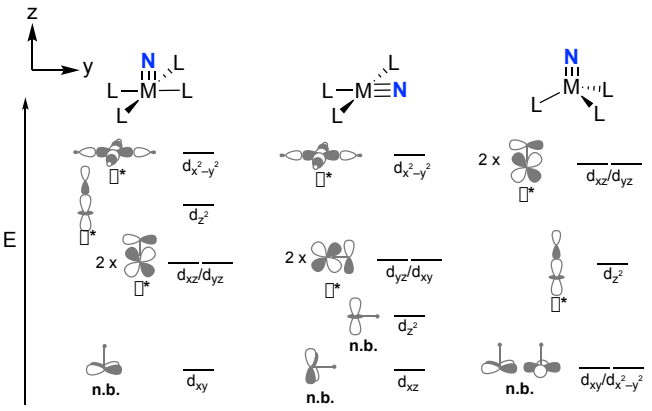

Figure 1. Qualitative molecular orbital diagram depicting the frontier d orbital interactions of terminal nitride complexes in SQPY (left), SQPL (middle), and Td (right) geometries (adapted from [7]).

Non-tetragonal systems adjacent to the nitrido wall have displayed reactivity toward small molecules, and examples are shown in Figure 2.[4, 8] For example, (PNP^{tBu})Os(N) (**A**)[8a] is representative of a class of pseudo-SQPL nitrides that are supported by pincer ligands (PNP^{tBu} = $N(CH_2CH_2P(^tBu)_2)_2^-$).[4, 7-9] In this geometry, both d_{z^2} and d_{xz} orbitals are nonbonding, and can accommodate the four d electrons (Figure 1, middle). **A** reacts with H_2 to form NH_3 by heterolytic addition of H_2 across the Os–N_{PNP} bond.[8b] Metal-nitrides have also been shown to react with a variety of main group electrophiles.[1e, 1f]

Finally and importantly, the use of nitrides to form N–C bonds represents a route to direct incorporation of N atoms into organic molecules. To our knowledge, the first report of reductive carbonylation of a terminal metal–nitride was in 2009.[10] Since then, there have been a few examples of nucleophilic Td, d^0 terminal metal–nitrides undergoing reductive carbonylation, including a N_2-derived terminal nitride (**B**).[11]

Another relevant example is the formally molybdenum(II) diphosphine-arene complex **C**.[12] It is the only known Mo nitride

with a d^4 configuration, and its nitride is much more reactive than higher-valent Mo nitrides. Its geometry deviates from the idealized geometries described above, leading to low-lying nonbonding Mo–$N_{nitride}$ orbitals that are reminiscent of the Td diagram in Figure 1. It also has η^4 coordination of an arene, which can accept electron density from the molybdenum. Despite these examples, there are not yet general guidelines of how to break through the nitrido wall to induce N–C bond forming reactions.

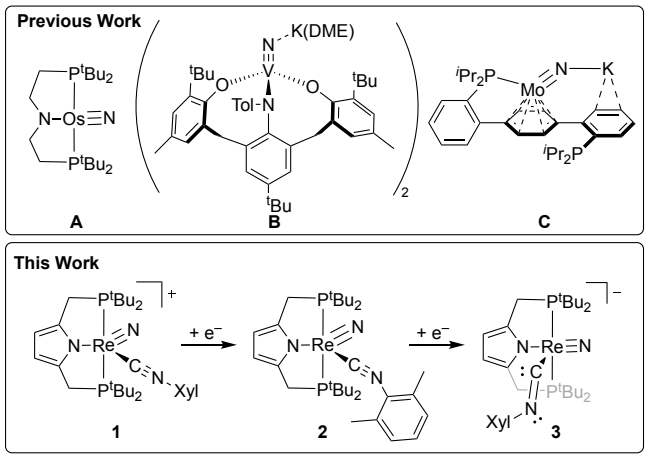

Figure 2. Selected examples of nitride complexes that display reactivity at the nitrido ligand.

Here, we show the exceptional capabilities of nitrides building from [(^{Pyrr}PNP)Re(N)(CNXyl)][PF_6] (**1**; ^{Pyrr}PNP = (2,5-{^{t}Bu$_2$PCH$_2$}$_2$C$_4$H$_2$N)$^-$, CNXyl = 2,6-dimethylphenyl isocyanide), a rhenium(V) complex where the nitride may be derived from N_2 splitting.[13] The cyclic voltammetry (CV) of **1** in fluorobenzene (FPh) indicated one reversible wave at –1.74 V and one quasi-reversible wave at –2.27 V (both versus $Fc^{+/0}$, Fc = ferrocene). These suggested that reduction of **1** might give isolable SQPY rhenium(IV) and rhenium(III) nitride complexes with formal d^3-d^4 configurations, which lie beyond the nitrido wall. Here, we describe the isolation of these compounds, and demonstrate that the CNXyl ligand stabilizes the reduced compounds by becoming non-innocent and adjusting its geometry and the geometry at Re. Further, it is an electron reservoir whose electrons can come back to the metal during a reaction with CO that forms a new N–C bond. In this way, we show that isocyanide co-ligands provide a potentially generalizable way to enhance the nucleophilicity of metal-nitrides and boost their utility in reaction sequences.

Results

Reduction of Nitride Complexes to form a Redox Series

Addition of 1.1 equiv of $CoCp^*_2$ to **1** in THF generated a blue paramagnetic product in 70% isolated yield. It was identified by single-crystal X-ray diffraction (XRD) as the formally rhenium(IV) complex (^{Pyrr}PNP)Re(N)(CNXyl) (**2**). The Re center has τ_5 = 0.18, indicating a pseudo-SQPY geometry with the nitrido ligand in the apical position. The Re–$N_{nitride}$ bond length of 1.700(7) Å is longer than in **1** (Table 1). Accordingly, the Re–$N_{nitride}$ stretching frequency of **2** is lower than that of **1**, at 995 cm^{-1} (964 cm^{-1} with Re–^{15}N) (Figure S51). Relative to **1**, the C–N_{CNXyl} bond length increases to 1.230(11) Å, the C–N–Xyl angle decreases to 140.6(8)°, and the C–N_{CNXyl} stretching mode shifts lower in energy to 1786 cm^{-1}, demonstrating greater backbonding into the π* orbital of the isocyanide.

Scheme 1. Synthesis of **2** from **1**.

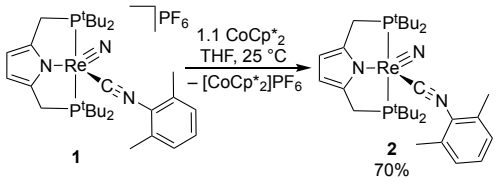

The room temperature solution magnetic moment[14] of **2** in C_6D_6 is 1.4 ± 0.1 μ_B, close to the expected spin-only value for a molecule with an *S* = 1/2 ground state (1.7 μ_B). The room temperature X-band EPR signals (g_{iso} = 2.025) of **2** and **2–^{15}N** in toluene are indistinguishable (Figure S49; the ^{15}N label is on the nitride). The signal can be fit with hyperfine coupling (HFC, A_{iso} = 276 MHz) to the $^{185/187}$Re center only. In other systems that display both metal and ligand radical character, the $^{185/187}$Re HFC was also found to be relatively small (A_{iso} < 400 MHz)[15] compared to compounds that lack ligand radical character (A_{iso} > 1000 MHz).[16] The small $^{185/187}$Re HFC observed for **2** suggests that the unpaired spin is delocalized and not solely on Re. Accordingly, the signal is somewhat broad, possibly indicating unresolved coupling to ^{31}P.

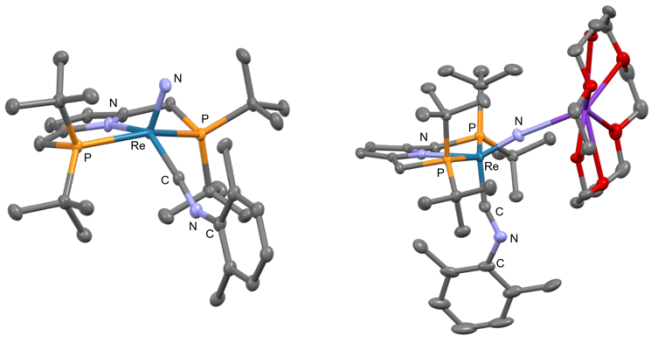

Figure 3. Solid-state structures of complexes **2** (left) and **3** (right) with thermal ellipsoids at 50% probability. Hydrogen atoms are omitted for clarity.

Table 1. Key stretching frequencies, bond distances and angles for **1**, **2**, and **3**.

	1[13]	**2**	**3**
ν_{Re-N} (cm^{-1})	1089, 1073	995	944
ν_{C-N} (cm^{-1})	2141	1786	1605
Re–$N_{nitride}$ (Å)	1.648(3)	1.700(7)	1.737(3)
Re–C_{CNXyl} (Å)	2.034(4)	1.921(8)	1.877(4)
Re–$N_{pyrrole}$ (Å)	2.053(3)	2.098(7)	2.227(3)
C–N–C_{CNXyl} (°)	171.4(4)	140.6(8)	124.5(4)

Scheme 2. Synthesis of **3** from **2**.

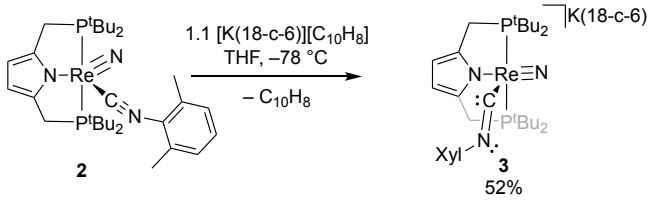

To access the product of the second reduction, 1 equiv of [K(18c6)][nap] (nap⁻ = naphthalenide) was added to **2** in THF at –78 ºC, which led to the formation of a dark yellow diamagnetic product in 52% yield (Scheme 2). XRD identified the formally rhenium(III) product as the anionic complex [(^{Pyrr}PNP)Re(N)(CNXyl)][K(18c6)] (**3**) (Figure 3). The nitrido ligand has moved from the apical position nearly into the plane of the ^{Pyrr}PNP ligand ($N_{pyrrole}$–Re–$N_{nitride}$ = 149.67(15)º), and the CNXyl ligand now occupies the apical position of the square pyramid (τ_5 = 0.03). The Re–$N_{nitride}$ bond length in **3** is further elongated to 1.737(3) Å, and the Re–$N_{nitride}$ stretching mode is at 944 cm^{-1} (920 cm^{-1} for Re–^{15}N), indicating a weakened bond. The C–N_{CNXyl} bond length is further increased to 1.278(6) Å, and the C–N–Xyl angle is 124.5(4)º, each indicating greater backbonding in **3** relative to **2** and **1**. Additionally, the CNXyl is now bent at the carbon atom, with a Re–C–N angle of 158.3(4)º. The IR spectrum of **3** shows bands at 1605 cm^{-1} and 1550 cm^{-1} (Figure S52). The signal at 1605 cm^{-1} is tentatively assigned to ν(C–N_{Xyl}) based on the DFT calculated stretching modes (Figure S94). The C–N_{Xyl} band in the IR spectrum of **3** lies at a lower energy than the analogous bands in **1** or **2** (shifts of 536 cm^{-1} and 181 cm^{-1}, respectively), corroborating the increase in backbonding from rhenium upon reduction observed in the crystal structure.

Overall, the reduction of **1** leads to isolable complexes with *formal* oxidation states of rhenium(IV) (**2**) and rhenium(III) (**3**), though the metrical and spectroscopic parameters indicate that charge is delocalized from the rhenium centers.

Computational Analysis of Bonding Interactions

In order to understand the changes in the Re-ligand bonding interactions across the redox series, we used density functional theory (DFT). Given the validation of BP86/TZVP(QZVP on Re) for (^{Pyrr}PNP)Re complexes,[13] we used the same method here. Geometry optimization for doublet **2** and singlet **3** gave good agreement with the XRD data: differences between computed and measured bond metrics all had < 3% deviation except for the C–N–Xyl angle of **3** which had a 5% deviation. The frequencies of the calculated C–N_{Xyl} stretching modes are 28 and 47 cm^{-1} from experimental values for **2** and **3**, respectively.

We used the Natural Bond Orbital (NBO) software package to illustrate the Lewis-like bonding interactions between Re and its ligands.[17] We began our investigation with the rhenium(V) nitride **1**. Not surprisingly, the calculated NBOs included three Re–$N_{nitride}$ bonds (two π and one σ), one Re–C_{CNXyl} bond (σ only), and three C–N_{CNXyl} bonds (two π and one σ) (Figure 4). These data are consistent with the expected Re–$N_{nitride}$ triple bond, a Re–C_{CNXyl} single bond and a C–N_{CNXyl} triple bond as described in the standard Lewis structure.

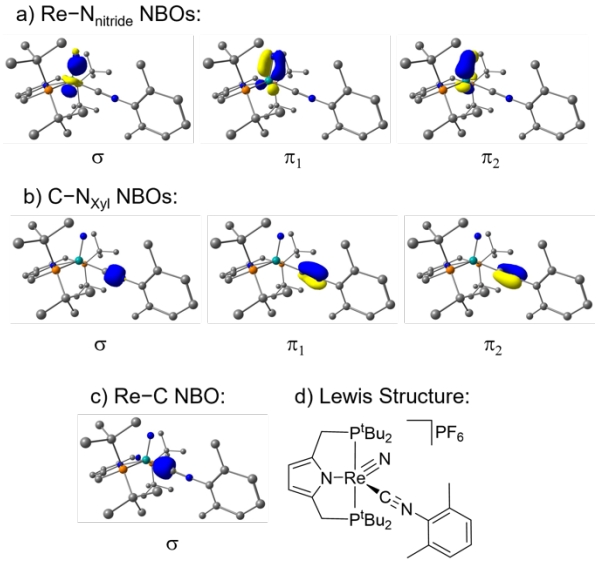

Figure 4. Calculated NBOs for **1** (contour value = 0.15 a.u.).

Next, we moved to the one-electron reduced compound **2**. Its SOMO (Figure 5a) and spin density (Figure 5b) are delocalized across the $N_{nitride}$–Re–CN_{CNXyl} fragment, and the SOMO is comprised of Re–$N_{nitride}$ π* and Re–C π orbitals. The α NBOs of **2** indicate two Re–$N_{nitride}$ bonds (one π and one σ), two Re–C_{CNXyl} bonds (one π and one σ), two C–N_{Xyl} bonds (one π and one σ), two lone pairs on $N_{nitride}$, and a single lone pair on N_{CNXyl} (Figure S100). On the other hand, the β NBOs for **2** are similar to **1**, and unlike the α NBOs. These results indicate "different structures for different spins" and spin polarization.[17] Additionally, there is a three-center four-electron interaction between one $N_{nitride}$ lone pair and the Re–C_{CNXyl} π bond in the α NBOs (Figure 5d). One depiction of the bonding is shown in Figure 5d, with a full Re–$N_{nitride}$ double bond, a full Re–C_{CNXyl} single bond, a full C–N_{Xyl} double bond, and additional delocalized bonding across the $N_{nitride}$–Re–CN_{Xyl} π system (see SI for additional details).

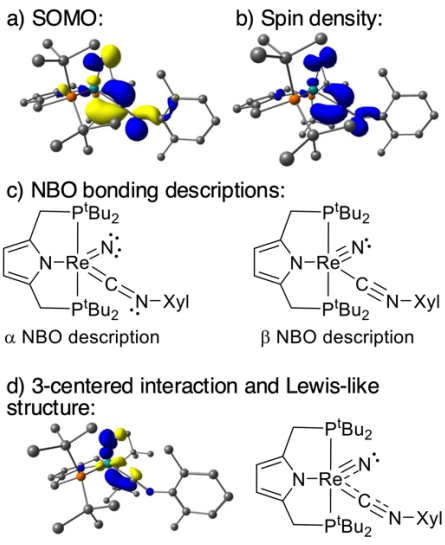

Figure 5. Computed SOMO (a), spin-density plot (b), NBO descriptions of one-electron α and β spin orbitals (c), and three-center interaction in the α NBOs between $N_{Nitride}$ LP and Re–C π bonding orbital and Lewis-like structure of nitride **2** (d). Contour values = 0.05, 0.005, and 0.15 a.u., respectively.

Reduction of **2** to **3** leads to distortion of the ReCNXyl unit in the DFT geometry optimizations like in the experimental X-ray crystal structure. The HOMO of **3** is delocalized across the $N_{nitride}$–Re–CNXyl π system and has Re–$N_{nitride}$ π* and Re–C π bonding character. The HOMO of **3** resembles the SOMO of **2** despite the geometric difference between the two complexes (Figure S99 and S101). Despite a longer Re–N distance and full occupancy of an orbital with some Re–$N_{nitride}$ π* character, NBO analysis of **3** indicates a Re–$N_{nitride}$ triple bond (two π and one σ) and a Re–C_{CNXyl} single bond (σ only) (Figure S103). However, the CNXyl ligand has been reduced by two electrons. The isocyanide NBOs feature two C–N_{CNXyl} bonds (one π and one σ) and a lone pair on both C and N atoms (Figure 6). Based on these computational data, the formally d^4 rhenium(III) species **3** is more accurately described as a d^2 rhenium(V) complex with a reduced $CNXyl^{2-}$ ligand.

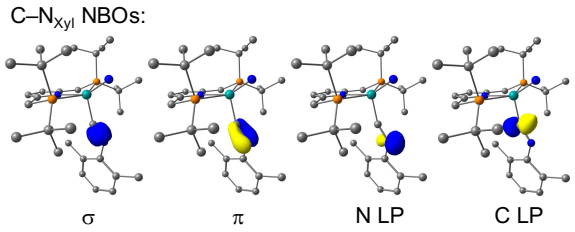

Figure 6. Calculated CNXyl NBOs for **3** (contour value = 0.15 a.u.).

Scheme 3. Synthesis of **4** and **5** from **3**.

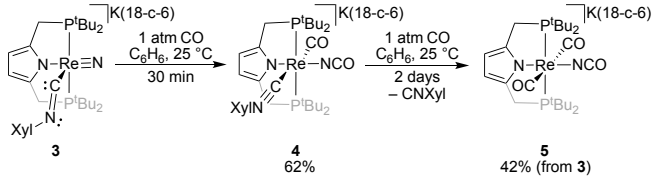

Reactions with CO Display the Nucleophilicity of the Reduced Rhenium Nitride

Introduction of a CO atmosphere to a solution of **3** in benzene at room temperature led to a color change from dark yellow to purple over 1 h, and then over the next 2 days the color changed to red. Both the purple and red species were crystallized (62% and 42% yield, respectively), and XRD identified them as the isocyanate products [(^{Pyrr}PNP)Re(NCO)(CO)(CNXyl)][K(18-c-6)] (**4**) and [(^{Pyrr}PNP)Re(NCO)(CO)$_2$][K(18-c-6)] (**5**) (Scheme 3 and Figure 7). Efforts were made to experimentally query the mechanism of N−C bond formation, but the results were not conclusive (see SI).

In **4**, the isocyanate ligand is *trans* to the pyrrole ring, similar to the position of the nitride in **3**. The CO and CNXyl ligands are *cis* to the PNP donors, and *trans* to one another. NOESY NMR experiments at −70 °C displayed cross peaks between the pincer ^{t}Bu groups and the CNXyl methyl groups (Figure S14), consistent with the crystallographically observed *cis* relationship.[18] An IR spectrum of **4** showed intense bands at 2250, 2036, 2006, and 1798 cm^{-1}. The ^{13}CO isotopologue, **4-^{13}CO** displayed isotopic shifts of the peaks at 2250 and 1798 cm^{-1} to 2201 and 1749 cm^{-1}, leading us to assign these to the isocyanate and the CO, respectively (Figure S55). In comparison to these dramatic shifts, the peaks at 2036 and 2006 cm^{-1} shifted only slightly to 2028 and 1999 cm^{-1}, and are assigned to normal modes with mostly C–N_{CNXyl} character. The IR spectrum of the final isocyanate product **5** displays prominent bands at 2245, 1919, and 1784 cm^{-1}. The band at 2245 cm^{-1} (2230 cm^{-1} in Re–^{15}NCO) is consistent with the asymmetric stretching mode of an isocyanate[19] while the bands at 1919 and 1784 cm^{-1} can be attributed to the stretching modes of CO. The Re–N_{NCO} stretching mode was also identified as a band at 1270 cm^{-1} (1253 cm^{-1} for Re–^{15}N).

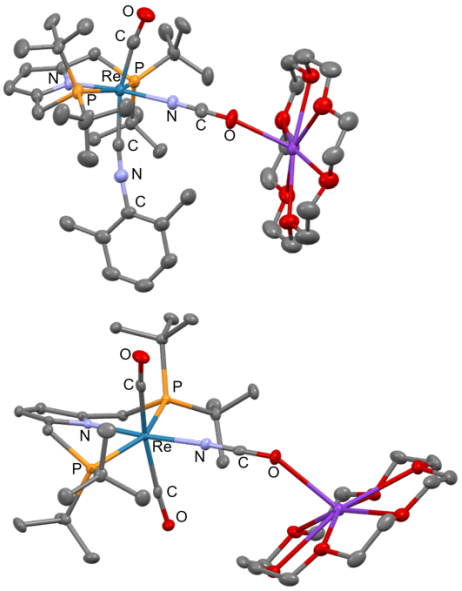

Figure 7. Solid-state structures of complex **4** (top) and **5** (bottom) with thermal ellipsoids at 50% probability. Hydrogen atoms and solvent molecules in the unit cell are omitted for clarity.

Scheme 4. Synthesis of **6** from **2**.

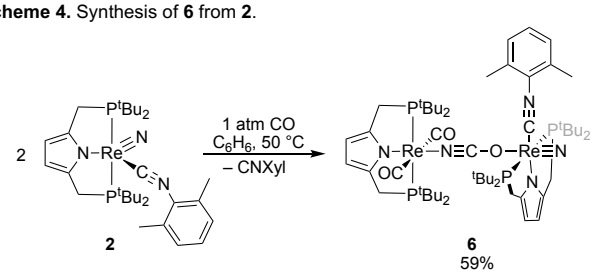

The reactivity of the neutral rhenium(IV) complex **2** with CO was also of interest. When an atmosphere of CO was introduced to a solution of **2** in benzene followed by heating at 50 °C for 12 hours, the solution changed from dark blue to orange. XRD identified the orange product as a cyanate-bridged bimetallic rhenium complex, [(^{Pyrr}PNP)Re(N)(CNXyl)](OCN)-[(^{Pyrr}PNP)Re(CO)$_2$] (**6**) (Scheme 4) (59% crystalline yield), in which one rhenium center retained its CNXyl ligand and nitride ligands, while the other rhenium center has two molecules of CO coordinated. Though we have not pursued mechanistic studies on this reaction, we speculate that in the presence of CO, **2** could disproportionate to a mixture of the cationic rhenium(V) complex **1** and a reduced rhenium complex. Disproportionation of **2** to form **3** and **1** is uphill by 12 kcal/mol, as calculated from the difference in $Re^{V/IV}$ and $Re^{IV/III}$ redox potentials, but this could still be accessible at higher temperature. As shown above, the reduced formally rhenium(III) complex **3** reacts with

CO to form the anionic rhenium(I) complex **5,** and consumption of **3** could drive the disproportionation to completion, giving one equiv of **1**. Then, since the anionic cyanate derived from **5** and the cationic **1** lack other counterions, they could bind to one another in the solid state to form the bimetallic Re^{V}-Re^{I} complex **6**. The NMR and IR spectra of **6** resemble a mixture of **1** and **5**, indicating that the two sides are electronically similar to the monometallic compounds, and supporting the rhenium(I)/rhenium(V) mixed-valence formulation (see SI).

Scheme 5. Computationally considered mechanistic pathways for CO addition to **3**. Free energies relative to **3** + 2 equiv CO are shown in parentheses, and computed transition state energies are shown under arrows in parentheses. In each structure, K(18-c-6) was modeled explicitly and is bound to the atom or group *trans* to the pyrrolyl nitrogen atom.

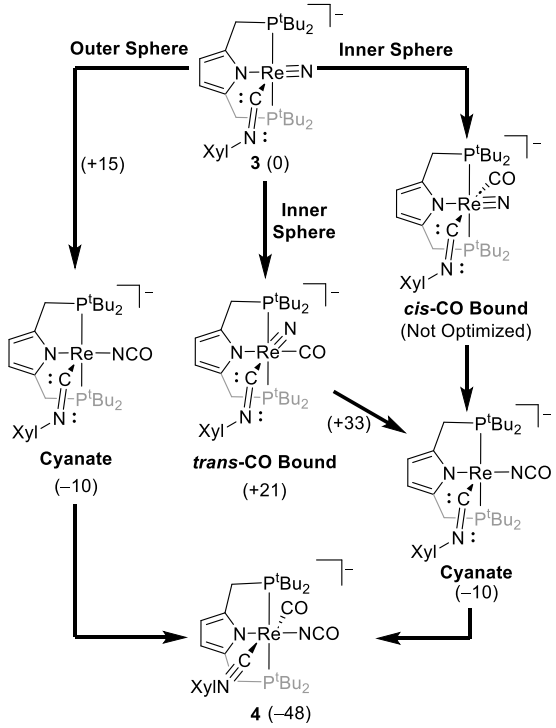

Computational Analysis of the N–CO Bond Formation Mechanism

We examined the potential mechanisms for addition of CO to **3** by DFT, namely an inner-sphere mechanism (CO coordination, then migration; right of Scheme 5) and an outer-sphere mechanism (direct attack of CO by nitride; left of Scheme 5). We modeled all species as spin singlets. To test the inner-sphere mechanism, we tried unsuccessfully to model a 6-coordinate structure in which CO binds *cis* to the pyrrolyl nitrogen (*cis*-CO Bound in Scheme 5). Attempted geometry optimizations of this species ejected CO to form the 5-coordinate isocyanate (see SI). This is unsurprising since coordination of the CO would generate a 20-electron complex. It was possible to optimize a different 6-coordinate structure in which CO coordinated between the nitrido ligand and the CNXyl such that the CO was *trans* to the PNP ligand (*trans*-CO Bound in Scheme 5). However, this structure was 21 kcal/mol uphill from **3**, which is higher than the barrier for direct N–C bond formation (see below). Therefore, it is not kinetically competent as a potential intermediate.

On the other hand, a direct N–CO bond formation was compatible with the rapid observed reaction (Figure 8). This elementary step is calculated to have a barrier of 15 kcal/mol leading to a five-coordinate isocyanate that lies downhill from **3** by 10 kcal/mol. The transition state has an angled approach of CO and the localized orbitals along the reaction coordinate show the movement of electrons from the nitride into the CO π^* orbitals and from CNXyl and the nitride into the metal center, corresponding with the formal reduction of the metal center to rhenium(I) (Figure S110).

Addition of a second equivalent of CO to form **4** is calculated to be downhill by an additional 38 kcal/mol, explaining why the 5-coordinate isocyanate is not observed experimentally. Overall, these computations support an outer-sphere mechanism of direct N–C bond formation through attack by a nucleophilic nitride directly on electrophilic CO, without pre-coordination of CO at the rhenium center.

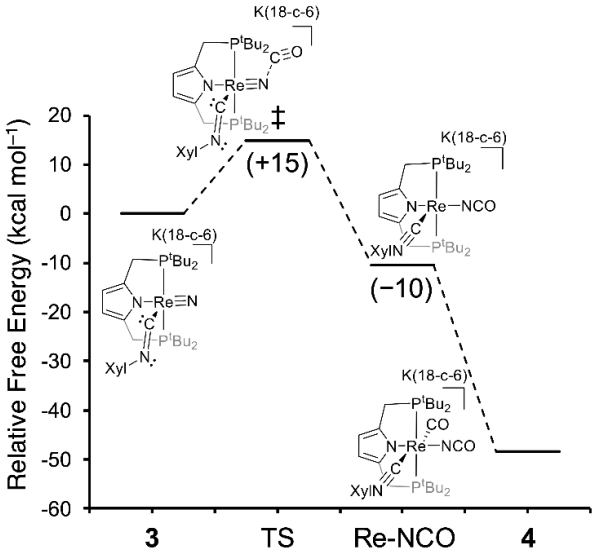

Figure 8. Free energy profile of the outer-sphere mechanism; energies are given relative to **3** + 2 CO in kcal/mol.

Discussion

Changes in Re–C and Re–N Bonding in the Redox Series

The rhenium-nitride complexes described here span the *formal* oxidation states rhenium(V) to rhenium(III), corresponding to d electron counts of two to four. The metrical and spectroscopic changes from **1** to **2** to **3** offer an opportunity to learn how the reduced metal nitride species are stabilized. First, compound **1** has slightly shorter Re–$N_{nitride}$ and Re–C_{CNR} bonds than the two other known rhenium(V)-nitride-isocyanide complexes.[20] Its C–N stretching frequency of 2141 cm^{-1} lies at a higher energy than free CNXyl (2119 cm^{-1}; 22 cm^{-1} difference). The C–N stretching frequency for another rhenium(V)-nitride-isocyanide was reported at 2172 cm^{-1} which is also shifted to a higher energy than its free ligand analogue at 2132 cm^{-1} (40 cm^{-1} difference).[20b] This is typical of low d electron count isocyanides, where binding shifts the band to higher energies by ~50–100 cm^{-1}.[21] This increase in the stretching frequency indicates that the isocyanide is acting primarily as a σ donor.[22] In **1**, the magnitude of the shift (22 cm^{-1}) is small, which suggests little backbonding.[23] The NBO analysis of **1** is consistent with the Gray-Ballhausen qualitative MO diagram for a SQPY nitride in that there is a triple bond to the nitride. Therefore, reduction of **1** to **2** would be expected to populate a Re–$N_{nitride}$ π* orbital. The 85 cm^{-1} shift to lower energy of the Re–$N_{nitride}$ frequency from **1** to **2** indeed suggests weakening of the Re–N bond, but reduction has a more profound impact on the CNXyl ligand. The C–N_{Xyl} stretching frequency of is a remarkable 355 cm^{-1} lower than in **1**, the C–N–Xyl angle bends more than 30°, the C–N_{Xyl} bond elongates by more than 0.07 Å, and the Re–C bond contracts by more than 0.10 Å. These data suggest substantial backbonding from the Re center, which results in partial Re–C π bonding and the N_{CNXyl} becoming sp^2-hybridized.[24] Isocyanide bending is well established in the literature,[25] but the identity of the supporting ligand also can affect the C–N stretching mode.[26] The data presented here suggest that the CNXyl ligand stabilizes the lower oxidation state in **2** through strong backbonding.

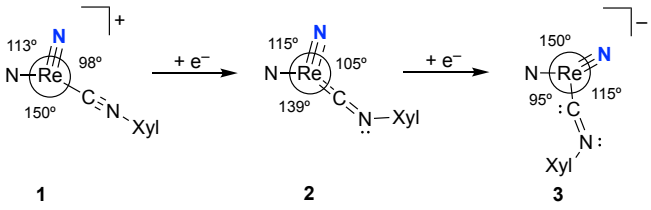

Figure 9. Nitride and isocyanide rotation about the Re center upon reduction.

The EPR signal for **2** shows a lower HFC to the Re nucleus than seen in typical rhenium(IV) compounds.[16b, 16c, 27] The calculated spin density plot and the three-center interaction from the α NBOs suggest delocalization of the unpaired spin across π orbitals of the entire N–Re–CNXyl core. The α and β NBOs for **2** are not co-localized; this situation is reminiscent of the allyl radical, where the α NBOs resemble the allyl anion, the β NBOs resemble the allyl cation, and the best bonding description is a hybrid of the two structures.[17] Together, these spectroscopic and computational results indicate that **2** is capable of breaking the nitrido wall by having the excess electron in an orbital that is not just on the nitride, but is also shared by the isocyanide.

In contrast to **1** and **2**, the nitride ligand of **3** moves closer to the pincer plane and the CNXyl ligand shifts into the apical position (Figure 9). The CNXyl ligand also becomes extremely distorted with a C–N–C_{Xyl} angle of 124.5(4)°, a C–N_{CNXyl} bond of 1.278(6) Å and C–N_{Xyl} stretching frequency of 1605 cm^{-1}. These metrics are comparable to the previously reported aminocarbyne (Figure 10, III) complex $[(dppe)_2Re(CNHMe)Cl][BF_4]$ (C–N–C_{Me} angle of 123(2)°, a ν_{C-N} of 1575 cm^{-1}, C–N bond length of 1.35(3) Å) despite the isocyanide N in **3** being only monosubstituted.[28] A similar comparison could be drawn between **3** and some iminoacyl complexes (Figure 10, IV).[29] Our NBO analysis of **3** suggests that despite being more reduced than **2**, rearrangement of the nitride and CNXyl ligands retains the full Re–$N_{nitride}$ triple bond, but has two lone pairs localized on C and N of the CNXyl ligand. The absence of an NBO with Re–C_{CNXyl} π bonding suggests that the Lewis structure V (Figure 10) most accurately describes **3**. This assignment requires a formal two electron reduction of the isocyanide ligand. Thus while compound **3** is *formally* d^4 rhenium(III), it is better described as d^2 rhenium(V). The assignment as rhenium(V) is bolstered by the chemical shift of the supporting ligand in the $^{31}P\{^1H\}$ NMR spectrum at 85.8 ppm, which is in the region of other rhenium(V)-nitride complexes bearing phosphine ligands (79.1 ppm for (^{Pyrr}PNP)Re(N)Cl and 96.8 ppm for **1**). In contrast, reported shifts for (PNP)Re^{III} compounds are all further upfield at 40 ppm or lower.[30]

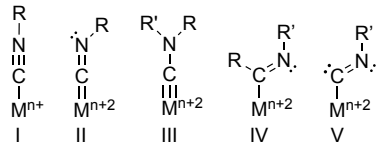

Figure 10. Lewis structures for various degrees of isocyanide weakening and activation.

Comparison Between d^4 Complexes with Nitride and Isocyanide Ligands

Most five-coordinate terminal nitrido complexes adopt SQPY geometries and have formal d electron counts of two or less as expected from the GB model.[1f] One reported series of ^{u}PNP^{tBu} pincer osmium complexes demonstrates both four and five coordinate nitrides with d^4 configurations (^{u}PNP = $N(CHCH^tBu_2)_2^-$.[4] The five-coordinate chloride precursor, [(^{u}PNP)Os(N)Cl][PF_6] (**D**; Figure 11), exhibits the expected SQPY geometry for a d^2 nitride, but two-electron reduction forms a SQPL product (^{u}PNP)Os(N) (**E**) as predicted by the qualitative MO diagram in Figure 1. Addition of CN^{t}Bu to **E** leads to the formation of the thermally unstable, five coordinate d^4 Os nitride, (^{u}PNP)Os(N)(CNtBu) (**F**). **F** was the only reported example of a five-coordinate d^4 nitride complex to break the nitrido wall.

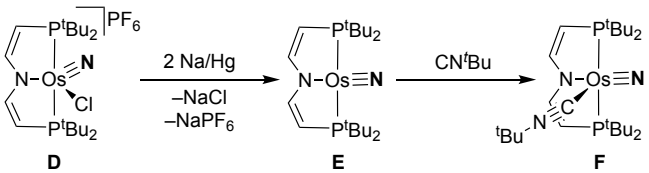

Figure 11. Synthesis of a five-coordinate Os^{+4} nitride supported by ^{u}PNP.[4]

Although **3** and **F** are isoelectronic, they exhibit very different isocyanide backbonding. Nitride **F** has a much shorter C–N_{CNtBu} bond length of 1.175(3)/1.180(3) Å, longer C–N–C_{tBu} angle of 155º/161º), and higher ν(C–N_{CNtBu}) of 2007 cm^{-1} suggesting that the isocyanide is not accepting as much electron density. In the osmium case, bending at C_{CNtBu} was described as being required to avoid σ conflict that would arise from the CN^{t}Bu lone pair interacting with a filled d_z^2 orbital. To avoid this conflict, the filled d_z^2 orbital can π-backbond into the unoccupied π^*-orbital of CN^{t}Bu (Figure 12, Model A). This contrasts with **3**, in which the significant distortion of the CNXyl ligand warrants the alternative explanation depicted in Figure 12 where the CNXyl ligand is best described as the dianion (Model B). In Model B, there is no need to avoid a σ conflict as the d_z^2 orbital in **3** is unoccupied. The difference between preferred bonding models in **F** vs. **3** may be attributed to the lower electronegativity of rhenium, which leads to stronger backbonding, and to the charge-stabilizing effect of the Xyl ring in conjugation with the isocyanide multiple bond.

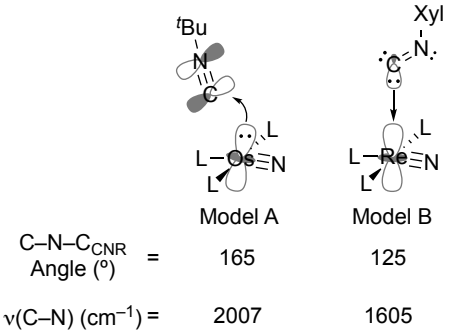

Figure 12. Different bonding models for the observed C_{CNR} bending.

Reactivity with Carbon Monoxide

A number of transition metal and actinide nitride complexes have been observed to react with CO to form cyanate or isocyanate,[31] but here we review the reactivity of only terminal nitride complexes to provide context.[8b, 10-12, 20b, 32] In general, a terminal nitride can react with CO through either outer-sphere attack on CO by the nitride or through inner-sphere coordination of CO followed by subsequent N−C coupling. With Td, d^0 nitrides, the sterics of the supporting ligands have been seen as the most important determinant of the mechanism. Metal centers with bulky supporting ligands typically proceed through outer sphere, nucleophilic attack of the nitride on CO; this applies to the vanadium–nitrides in the middle of Figure 2 and Figure 13 (**G**).[10, 11b] With less sterically demanding ligands, an inner-sphere mechanism is observed, as with nitride **H** in Figure 13.[11a] A computational comparison of nitrides **H** and **I** further supported the dependence of the mechanism on the sterics of the supporting ligands.[32b] Ti nitrides can also react as nucleophiles toward CO, as demonstrated by the reactivity of an anionic titanium(IV)–nitride (**L** in Figure 14).[32c] The d^4 Td iron(IV)–nitride **J** (Figure 14) formed isocyanide through an outer-sphere mechanism, but in this case the nitride acted as an electrophile toward CO.[32d]

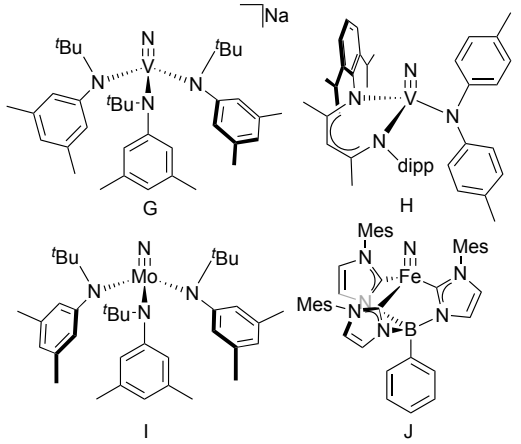

Figure 13. Selected examples of Td metal–nitrides that form NCO^-. Mes = 2,4,6-$Me_3C_6H_2$.

Moving to SQPY complexes, a tungsten complex **K** split dinitrogen to form d^2 tungsten(IV) terminal nitrides (PNP^{tBu})W(N)(CO) that reacted with CO to yield free cyanate.[32a] In this case, the mechanism was shown by isotope labeling to be an inner sphere pathway in which the pre-associated CO carbonylates the nitride, followed by coordination of two CO molecules.

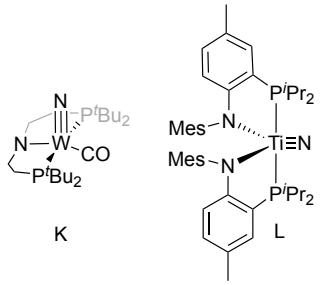

Figure 14. SQPY metal–nitrides that react to form NCO^-.

Beyond Td geometries, a SQPL d^4 ruthenium(IV)–nitride **M** with a PNP^{tBu} pincer supporting ligand was computed to undergo isocyanate formation via outer sphere, direct nucleophilic attack on CO (**M** in Figure 15).[8b] The formally molybdenum(II) diphosphine-arene complex described above (**C** in Figure 15) also reacts with CO to form NCO^-.[12] Isotope labeling experiments indicated that the mechanism is most likely outer-sphere.

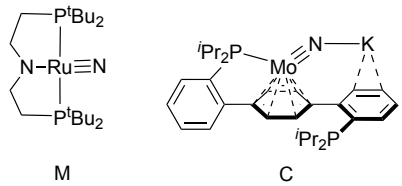

Figure 15. SQPL Ru–nitride and Mo–nitride complexes that react to form NCO^-.

Nitride **3** is *formally* a d^4 system like **M** and **C**, but avoids the buildup of electron density at the metal by storing the additional electrons in the CNXyl ligand, and thus it is best viewed as rhenium(V)/$CNXyl^{2-}$. However, many of the bonding orbitals are delocalized throughout the N_{Xyl}–C–Re–$N_{nitride}$ unit, providing a path for the electrons stored in $CNXyl^{2-}$ to return to the metal center. When CO is introduced, the nitride interacts with the π^*

orbital of CO to allow direct (outer-sphere) N–C bond formation, followed by electron flow from CNXyl to rhenium as the NCO ligand forms its final geometry. This rapid reaction to form **4** is followed by a slow replacement of isocyanide by CO to form **5**.
A compelling aspect of the redox series **1**–**3** is that isocyanide ligands are easily introduced into coordination complexes, and may be a generalizable method for enabling unreactive terminal nitride complexes (including those derived from N_2 splitting, as done here) to have accessible reduced forms that can undergo reactivity with electrophiles. Though the specific reaction described here leads ultimately to a rhenium-carbonyl complex that is not amenable to completion of a catalytic cycle, it reinforces the value of isocyanides as supporting ligands.[33]

Conclusions

We show rhenium-nitride-isocyanide complexes that span three formal oxidation states and avoid the "nitrido wall" by delocalizing electrons throughout the N–Re–CNXyl core. The formally Re(IV) complex **2** uses a Re–CNXyl π backbonding interaction to move some electron density in the SOMO off the Re center. Further reduction to **3** results in greater delocalization of electron density into the CNXyl ligand, and the product is best described as a rhenium(V) nitride despite its formal rhenium(III) oxidation state. Even though it bypasses the "nitrido wall" by moving electrons to the isocyanide, they can return when the nitride ligand engages in nucleophilic reactivity with CO. In another recent study, we showed that the use of isocyanide as a second supporting ligand in this Re system enables PCET to the nitride to form ammonia.[13] Here, deeper reduction is also accommodated, making the nitride electron-rich enough for attack on CO to form N–C bonds from an N_2-derived nitride. This series of reactions sums to the conversion of N_2 and CO to NCO^-.

Acknowledgements

This work was supported by the U.S. National Science Foundation (CHE-1954254 to P.L.H. and DGE-1752134 to J.E.W.). This research made use of the Chemical and Biophysical Instrumentation Center at Yale University (RRID:SCR_021738). We thank Alexander Miller and Alan Goldman for helpful discussions.

Keywords: Rhenium • nitride • cyanate • isocyanide

References

[1] a) W. P. Griffith, *Coord. Chem. Rev.* **1972**, *8*, 369-396; b) J. F. Berry, *Comments Inorg. Chem.* **2009**, *30*, 28-66; c) K. Dehnicke, J. Strähle, *Angew. Chem., Int. Ed.* **1981**, *20*, 413-426; d) K. Dehnicke, J. Strähle, *Angew. Chem., Int. Ed.* **1992**, *31*, 955-978; e) S. J. K. Forrest, B. Schluschaß, E. Y. Yuzik-Klimova, S. Schneider, *Chem. Rev.* **2021**, *121*, 6522-6587; f) R. A. Eikey, M. M. Abu-Omar, *Coord. Chem. Rev.* **2003**, *243*, 83-124; g) S. Kim, F. Loose, P. J. Chirik, *Chem. Rev.* **2020**, *120*, 5637-5681; h) J. M. Smith, *Progr. Inorg. Chem.* **2014**, *58*, 417-470.

[2] a) M. P. Shaver, M. D. Fryzuk, *Adv. Synth. Catal.* **2003**, *345*, 1061-1076; b) M. J. Trenerry, C. M. Wallen, T. R. Brown, S. V. Park, J. F. Berry, *Nat. Chem.* **2021**, *13*, 1221-1227; c) F. Schendzielorz, M. Finger, J. Abbenseth, C. Würtele, V. Krewald, S. Schneider, *Angew. Chem., Int. Ed.* **2019**, *58*, 830-834; d)J. J. Curley, E. L. Sceats, C. C. Cummins, *J. Am. Chem. Soc.* **2006**, *128*, 14036-14037; e) J.-P. F. Cherry, A. R. Johnson, L. M. Baraldo, Y.-C. Tsai, C. C. Cummins, S. V. Kryatov, E. V. Rybak-Akimova, K. B. Capps, C. D. Hoff, C. M. Haar, S. P. Nolan, *J. Am. Chem. Soc.* **2001**, *123*, 7271-7286.

[3] a) C. J. Ballhausen, H. B. Gray, *Inorg. Chem.* **1962**, *1*, 111-122; b) W. A. Nugent, J. M. Mayer, *Metal-Ligand Multiple Bonds*, Wiley, New York, 1988. c) J. R. Winkler, H. B. Gray, in *Molecular Electronic Structures of Transition Metal Complexes I* (Eds.: D. M. P. Mingos, P. Day, J. P. Dahl), Springer Berlin Heidelberg, Berlin, Heidelberg, **2012**, pp. 17-28.

[4] J. Abbenseth, S. C. Bete, M. Finger, C. Volkmann, C. Würtele, S. Schneider, *Organometallics* **2018**, *37*, 802-811.

[5] L. Bonomo, E. Solari, R. Scopelliti, C. Floriani, *Angew. Chem., Int. Ed.* **2001**, *40*, 2529-2531.

[6] H.-C. Chang, Y.-H. Lin, C. Werlé, F. Neese, W.-Z. Lee, E. Bill, S. Ye, *Angew. Chem., Int. Ed.* **2019**, *58*, 17589-17593.

[7] M. G. Scheibel, B. Askevold, F. W. Heinemann, E. J. Reijerse, B. de Bruin, S. Schneider, *Nat. Chem.* **2012**, *4*, 552-558.

[8] a) F. S. Schendzielorz, M. Finger, C. Volkmann, C. Würtele, S. Schneider, *Angew. Chem., Int. Ed.* **2016**, *55*, 11417-11420; b) B. Askevold, J. T. Nieto, S. Tussupbayev, M. Diefenbach, E. Herdtweck, M. C. Holthausen, S. Schneider, *Nat. Chem.* **2011**, *3*, 532-537.

[9] M. Kinauer, M. Diefenbach, H. Bamberger, S. Demeshko, E. J. Reijerse, C. Volkmann, C. Würtele, J. van Slageren, B. de Bruin, M. C. Holthausen, S. Schneider, *Chem. Sci.* **2018**, *9*, 4325-4332.

[10] J. S. Silvia, C. C. Cummins, *J. Am. Chem. Soc.* **2009**, *131*, 446-447.

[11] a) B. L. Tran, M. Pink, X. Gao, H. Park, D. J. Mindiola, *J. Am. Chem. Soc.* **2010**, *132*, 1458-1459; b) Y. Ishida, H. Kawaguchi, *J. Am. Chem. Soc.* **2014**, *136*, 16990-16993.

[12] J. A. Buss, C. Cheng, T. Agapie, *Angew. Chem., Int. Ed.* **2018**, *57*, 9670-9674.

[13] J. E. Weber, N. D. McMillion, A. S. Hegg, A. E. Wertz, M. Aliahmadi, B. Q. Mercado, R. H. Crabtree, H. S. Shafaat, A. J. M. Miller, P. L. Holland, *J. Am. Chem. Soc.* **2024**, *146*, 33595-33607.

[14] D. F. Evans, *J. Chem. Sci.* **1959**, 2003-2005.

[15] a) L. Alig, K. A. Eisenlohr, Y. Zelenkova, S. Rosendahl, R. Herbst-Irmer, S. Demeshko, M. C. Holthausen, S. Schneider, *Angew. Chem., Int. Ed.* **2022**, *61*, e202113340; b) S. Frantz, J. Fiedler, I. Hartenbach, T. Schleid, W. Kaim, *J. Organomet. Chem.* **2004**, *689*, 3031-3039; c) A. Klein, C. Vogler, W. Kaim, *Organometallics* **1996**, *15*, 236-244; d) T. Scheiring, A. Klein, W. Kaim, *J. Chem. Soc., Perkin Trans. II* **1997**, 2569-2572.

[16] a) A. H. Al-Mowali, A. L. Porte, *J. Chem. Soc., Dalton Trans.* **1975**, 50-55; b) R. F. Bufaical, E. A. Harris, *Solid State Commun.* **1981**, *39*, 1143-1146; c) S. K. Singh, G. Rajaraman, *Nat. Commun.* **2016**, *7*, 10669.

[17] a) J. E. D. Glendening, K. Badenhoop, A. E. Reed, J. E. Carpenter, J. A. Bohmann, C. M. Morales, P. Karafiloglou, C. R. Landis, and F. Weinhold, *NBO 7.0*, Theoretical Chemistry Institute, University of Wisconsin, Madison, **2018**. b) F. Weinhold, J. E. Carpenter, "The Natural Bond Orbital Lewis Structure Concept For Molecules, Radicals, and Radical Ions," in *The Structure of Small Molecules and Ions* (R. Naaman, Z. Vager, eds), Plenum, New York, 1988, pp. 227-236. Online at https://www.researchgate.net/profile/Frank_Weinhold/publication/285067148_The_Natural_Bond_Orbital_Lewis_Structure_Concept_for_Molecules_Radicals_and_Radical_Ions/links/565da5cb08aefe619b266148/The-Natural-Bond-Orbital-Lewis-Structure-Concept-for-Molecules-Radicals-and-Radical-Ions.pdf (accessed April 15, 2025).

[18] K. R. Williams, R. W. King, *J. Chem. Educ.* **1990**, *67*, A125.

[19] R. A. Bailey, S. L. Kozak, T. W. Michelsen, W. N. Mills, *Coord. Chem. Rev.* **1971**, *6*, 407-445.

[20] a) N. S. Lambic, R. D. Sommer, E. A. Ison, *Dalton Trans.* **2020**, *49*, 6127-6134; b) N. S. Lambic, R. D. Sommer, E. A. Ison, *Dalton Trans.* **2018**, *47*, 758-768.

[21] a) T. J. Morsing, J. Bendix, *J. Mol. Struct.* **2013**, *1039*, 107-112; b) G. Claude, F. Salsi, A. Hagenbach, M. Gembicky, M. Neville, C. Chan, J. S. Figueroa, U. Abram, *Organometallics* **2020**, *39*, 2287-2294.

[22] a) A. S. Goldman, K. Krogh-Jespersen, *J. Am. Chem. Soc.* **1996**, *118*, 12159-12166. b) M. Finze, E. Bernhardt, A. Terheiden, M. Berkei, H. Willner, D. Christen, H. Oberhammer, F. Aubke, *J. Am. Chem. Soc.* **2002**, *124*, 15385-15398.

[23] a) H. S. La Pierre, J. Arnold, R. G. Bergman, F. D. Toste, *Inorg. Chem.* **2012**, *51*, 13334-13344; b) H. Kropp, A. Scheurer, F. W. Heinemann, J. Bendix, K. Meyer, *Inorg. Chem.* **2015**, *54*, 3562-3572; c) T. L. Gianetti, N. C. Tomson, J. Arnold, R. G. Bergman, *J. Am. Chem. Soc.* **2011**, *133*, 14904-14907.

[24] a) K. L. Engelman, P. S. White, J. L. Templeton, *Organometallics* **2010**, *29*, 4943-4949; b) F. A. Cotton, F. Zingales, *J. Am. Chem. Soc.* **1961**, *83*, 351-355.

[25] a) A. J. L. Pombeiro, M. F. C. Guedes da Silva, R. A. Michelin, *Coord. Chem. Rev.* **2001**, *218*, 43-74; b) R. A. Michelin, A. J. L. Pombeiro, M. F. C. Guedes da Silva, *Coord. Chem. Rev.* **2001**, *218*, 75-112; c) V. P. Boyarskiy, N. A. Bokach, K. V. Luzyanin, V. Y. Kukushkin, *Chem. Rev.* **2015**, *115*, 2698-2779.

[26] F. Salsi, M. Neville, M. Drance, A. Hagenbach, C. Chan, J. S. Figueroa, U. Abram, *Chem. Commun.* **2020**, *56*, 7009-7012.

[27] J. Martínez-Lillo, T. F. Mastropietro, E. Lhotel, C. Paulsen, J. Cano, G. De Munno, J. Faus, F. Lloret, M. Julve, S. Nellutla, J. Krzystek, *J. Am. Chem. Soc.* **2013**, *135*, 13737-13748.

[28] A. J. L. Pombeiro, M. F. N. N. Carvalho, P. B. Hitchcock, R. L. Richards, *J. Chem. Soc., Dalton Trans.* **1981**, 1629-1634.

[29] a) G. R. Owen, R. Vilar, A. J. P. White, D. J. Williams, *Organometallics* **2002**, *21*, 4799-4807; b) S. P. Semproni, W. S. McNeil, R. A. Baillie, B. O. Patrick, C. F. Campana, P. Legzdins, *Organometallics* **2010**, *29*, 867-875.

[30] a) I. Klopsch, M. Finger, C. Würtele, B. Milde, D. B. Werz, S. Schneider, *J. Am. Chem. Soc.* **2014**, *136*, 6881-6883; b) G. P. Connor, D. Delony, J. E. Weber, B. Q. Mercado, J. B. Curley, S. Schneider, J. M. Mayer, P. L. Holland, *Chem. Sci.* **2022**, *13*, 4010-4018; c) R. S. van Alten, P. A. Wieser, M. Finger, J. Abbenseth, S. Demeshko, C. Würtele, I. Siewert, S. Schneider, *Inorg. Chem.* **2022**, *61*, 11581-11591.

[31] a) S. P. Semproni, P. J. Chirik, *Angew. Chem., Int. Ed.* **2013**, *52*, 12965-12969; b) S. P. Semproni, C. Milsmann, P. J. Chirik, *Angew. Chem., Int. Ed.* **2012**, *51*, 5213-5216; c) L. Barluzzi, L. Chatelain, F. Fadaei-Tirani, I. Zivkovic, M. Mazzanti, *Chem. Sci.* **2019**, *10*, 3543-3555.

[32] a) B. Schluschaß, J.-H. Borter, S. Rupp, S. Demeshko, C. Herwig, C. Limberg, N. A. Maciulis, J. Schneider, C. Würtele, V. Krewald, D. Schwarzer, S. Schneider, *JACS Au* **2021**, *1*, 879-894; b) A. F. Cozzolino, J. S. Silvia, N. Lopez, C. C. Cummins, *Dalton Trans.* **2014**, *43*, 4639-4652; c) M. Bhunia, C. Sandoval-Pauker, D. Fehn, L. N. Grant, S. Senthil, M. R. Gau, A. Ozarowski, J. Krzystek, J. Telser, B. Pinter, K. Meyer, D. J. Mindiola, *Angew. Chem., Int. Ed.* **2024**, *63*, e202404601; d) J. J. Scepaniak, R. P. Bontchev, D. L. Johnson, J. M. Smith, *Angew. Chem., Int. Ed.* **2011**, *50*, 6630-6633; e) P. A. Cleaves, D. M. King, C. E. Kefalidis, L. Maron, F. Tuna, E. J. L. McInnes, J. McMaster, W. Lewis, A. J. Blake, S. T. Liddle, *Angew. Chem., Int. Ed.* **2014**, *53*, 10412-10415.

[33] a) A. E. Carpenter, C. E. Moore, A. L. Rheingold, J. S. Figueroa, *Organometallics* **2021**, *40*, 968-978; b) M. R. Gau, T. M. Keller, J. J. Scepaniak, *Eur. J. Inorg. Chem.* **2024**, *27*, e202400146; c) F. E. Hahn, *Angew. Chem. Int. Ed.* **1993**, *32*, 650-665; d) M. Knorn, E. Lutsker, O. Reiser, *Chem. Soc. Rev.* **2020**, *49*, 7730-7752; e) F. Salsi, M. Neville, M. Drance, A. Hagenbach, C. Chan, J. S. Figueroa, U. Abram, *Chem. Commun.* **2020**, *56*, 7009-7012; f) L. Weber, *Angew. Chem. Int. Ed.* **1998**, *37*, 1515-1517.

[34] Deposition numbers 2420479 (for **2**), 2420480 (for **3**), 2420686 (for **4**), 2420481 (for **5**), 2420482 (for **6**), 2420483 (for [(^{pyrr}PNP)Re(N)(NCMe)][PF_6] – see SI), and 2420684 (for [(^{pyrr}PNP)Re(N)(CO)][PF_6] – see SI) contain the supplementary crystallographic data for this paper. These data are provided free of charge by the joint Cambridge Crystallographic Data Centre and Fachinformationszentrum Karlsruhe Access Structures service.

[35] M. Kreye, M. Freytag, P. G. Jones, P. G. Williard, W. H. Bernskoetter, M. D. Walter, *Chem. Commun.* **2015**, *51*, 2946-2949.

[36] J. L. Robbins, N. Edelstein, B. Spencer, J. C. Smart, *J. Am. Chem. Soc.* **1982**, *104*, 1882-1893.

[37] M. Castillo, A. J. Metta-Magaña, S. Fortier, *New J. Chem.* **2016**, *40*, 1923-1926.

[38] M. Krejčik, M. Daněk, F. Hartl, *J. Electroanal. Chem. Interfac. Electrochem.* **1991**, *317*, 179-187.

[39] J. E. Weber, F. Hasanayn, M. Fataftah, B. Q. Mercado, R. H. Crabtree, P. L. Holland, *Inorg. Chem.* **2021**, *60*, 6115-6124.

[40] R. A. Bailey, S. L. Kozak, T. W. Michelsen, W. N. Mills, *Coord. Chem. Rev.* **1971**, *6*, 407-445.

[41] A. Spek, *Acta Cryst. C* **2015**, *71*, 9-18.

[42] I. Guzei, *J. Appl. Cryst.* **2014**, *47*, 806-809.

[43] P. van der Sluis, A. L. Spek, *Acta Cryst. A* **1990**, *46*, 194-201.

[44] a) F. Neese, *WIREs Comput. Mol. Sci.* **2012**, *2*, 73-78; b) F. Neese, *WIREs Comput. Mol. Sci.* **2018**, *8*, e1327; c) F. Neese, *WIREs Comput. Mol. Sci.* **2022**, *12*, e1606; d) F. Neese, F. Wennmohs, U. Becker, C. Riplinger, *J. Chem. Phys.* **2020**, *152*.

[45] J. E. D. Glendening, K. Badenhoop, A. E. Reed, J. E. Carpenter, J. A. Bohmann, C. M. Morales, P. Karafiloglou, C. R. Landis, and F. Weinhold, *NBO 7.0*, Theoretical Chemistry Institute, University of Wisconsin, Madison, **2018**.

[46] *Chemcraft - graphical software for visualization of quantum chemistry computations.* Version 1.8, build 682.